Discharge-Stage Relationship on Urban Streams Evaluated at USGS Gauging Stations, St. Louis, Missouri

Robert E. Criss[1], **David L. Nelson**[2]

1. *Department of Earth and Planetary Sciences, Washington University, St. Louis MO 63130, USA*
2. *470 Columbia Cir, Pasadena CA 91105, USA*
Robert E. Criss: https://orcid.org/0000-0002-6484-1875

ABSTRACT: Extensive USGS data tables and detailed, 1 m^2 LiDAR surveys are used to determine the optimal power *n* that relates discharge (*Q*) to stage (*h**) above channel bottom (*h$_o$*) at 39 gauging stations on small streams in the St. Louis, Missouri area, all of which have catchments of 0.6 to 220 km^2. Four different methodologies are employed to determine both *n* and *h$_o$*: (1) optimizing linearity in a plot of *Q$^{1/n}$ vs.* local stage (*h$_L$*) using USGS field measurements at each site; (2) optimizing linearity in a plot of *Q$^{1/n}$ vs. h$_L$* using USGS rating tables at each site; (3) a mathematical inverse method applied to the same USGS rating tables; (4) use of LiDAR data on channel geometry to determine the power dependences of channel area *A* and hydraulic radius *H* on *h**, combined with the Manning and rational equations to predict *n*. Of these methods, only methods 2 and 3 compare favorably, and these values compare poorly with Method 1 based on field data, and with method 4 based on theoretical and empirical relationships. Because Method 4 is predictive, it provides a useful alternative to methods 1–3 that are based on USGS field measurements, which are heavily weighted toward low discharges. We conclude that the apparent values of *n* in the USGS rating tables are systematically too low for small streams.
KEY WORDS: stream gauging, LiDAR topography, urban flooding, discharge, hydrology.

0 INTRODUCTION

Flash flooding of small creeks in urban areas is of concern because flows and water levels are greatly increased by impervious cover, and the consequences are magnified by the proximity of valuable properties and large human populations (e.g., FEMA, 2015; Southard, 2010). Urban floodwaters also have poor water quality, because of contributions from combined sewer overflows, and runoff laden with road salt, bacteria, sediment, debris and other contaminants, so cleanup of damaged properties is both dangerous and expensive (MODNR, 2020; Hasenmueller and Criss, 2013). The St. Louis area, Missouri, has all of these problems, and several municipalities and agencies have taken extraordinary measures including massive improvements to sewer systems, ordinance changes, and buyouts to ameliorate them. Also among these measures is the monitoring of 39 USGS gauging stations installed on St. Louis streams (USGS, 2020), providing what may be the greatest concentration of detailed, publicly-available stream data in the world.

Water level and discharge are the basic descriptors of stream flow, and detailed knowledge of their interrelationship is essential to understanding flood dynamics. Water level (stage) is the key independent variable that is directly observed, and the parameter that is most directly related to local topography and flood damage. Discharge (flow rate) has practical importance in resource evaluation, and has scientific importance because it is closely related to precipitation delivery and watershed character. However, unlike stage, which is easily and accurately measured, discharge is a dependent variable that must be calculated from detailed measurements of channel area and water velocity (e.g., Wahl et al., 1995). In practice, measurements made at or near gauging stations during multiple site visits are used to calibrate rating tables for any given site, which are then used to estimate discharge from the stage, whose continuous measurement has become routine.

The wealth of data available for the St. Louis area provides a special opportunity to evaluate the discharge-stage relationship and the underlying dynamics. This paper provides several novel computational and mathematical techniques to glean insights from this unique dataset. We are surprised to find little consistency in the results for different sites, and internal disagreements at many single sites, enabling us to offer some recommendations.

1 REGIONAL HYDROGEOLOGIC SETTING

The combined 1 680 km^2 area of St. Louis County and the City of St. Louis, hereafter called the "St. Louis region", is located near the famous confluence of the Missouri and Mississippi Rivers. These great rivers respectively form the northern and eastern boundaries of this area, which also hosts the lowermost reach of the much smaller Meramec River, which constitutes much of the southern border (Fig. 1). The uplands of

---

the area are located in the Ozark border physiographic province (Vineyard, 1967), providing moderate topographic relief and elevations that range from about 110 to 250 m. These uplands are dissected by several creeks whose watersheds are as large as 120 km^2, but several of these flow into the River des Peres, a highly channelized local stream that drains a combined area of ~290 km^2 (ASCE, 1988).

Much of the St. Louis region is underlain by Mississippian limestone, but its north-central part is underlain by Pennsylvanian clastic formations, and bedrock in the southwestern part is dominated by Ordovician limestones and dolostones (Harrison, 1997). Karst features are common in many of the limestone units, particularly in sinkhole plains near the Mississippi River, and while subsurface drainage remains significant, many karst features have been obliterated by urban development (Criss et

al., 2007). As much as 10 m of Pleistocene loess caps bedrock in much of the area (Lutzen and Rockaway, 1989).

Regional flooding of large rivers and flash flooding of small creeks are significant hazards in the region, but only small streams are considered below. St. Louis rainfall averages 96 cm/y, but an average of 107 cm/y has been received since 1998 when most of the stream data under consideration were collected, and a record of 155.5 cm was delivered in 2015 (NWS, 2020). More significant is that sharp convective storms deliver >3 cm/h more than once per year (NOAA, 2017). The time constants for response of the small urban streams in this area are very short, typically <30 min, providing creek flows that commonly exceed 100 m^3/s, representing 1 000–3 000 times their average flows (Criss, 2018). Concomitant creek stages rise rapidly to hazardous levels, at rates that can exceed 3 m/h.
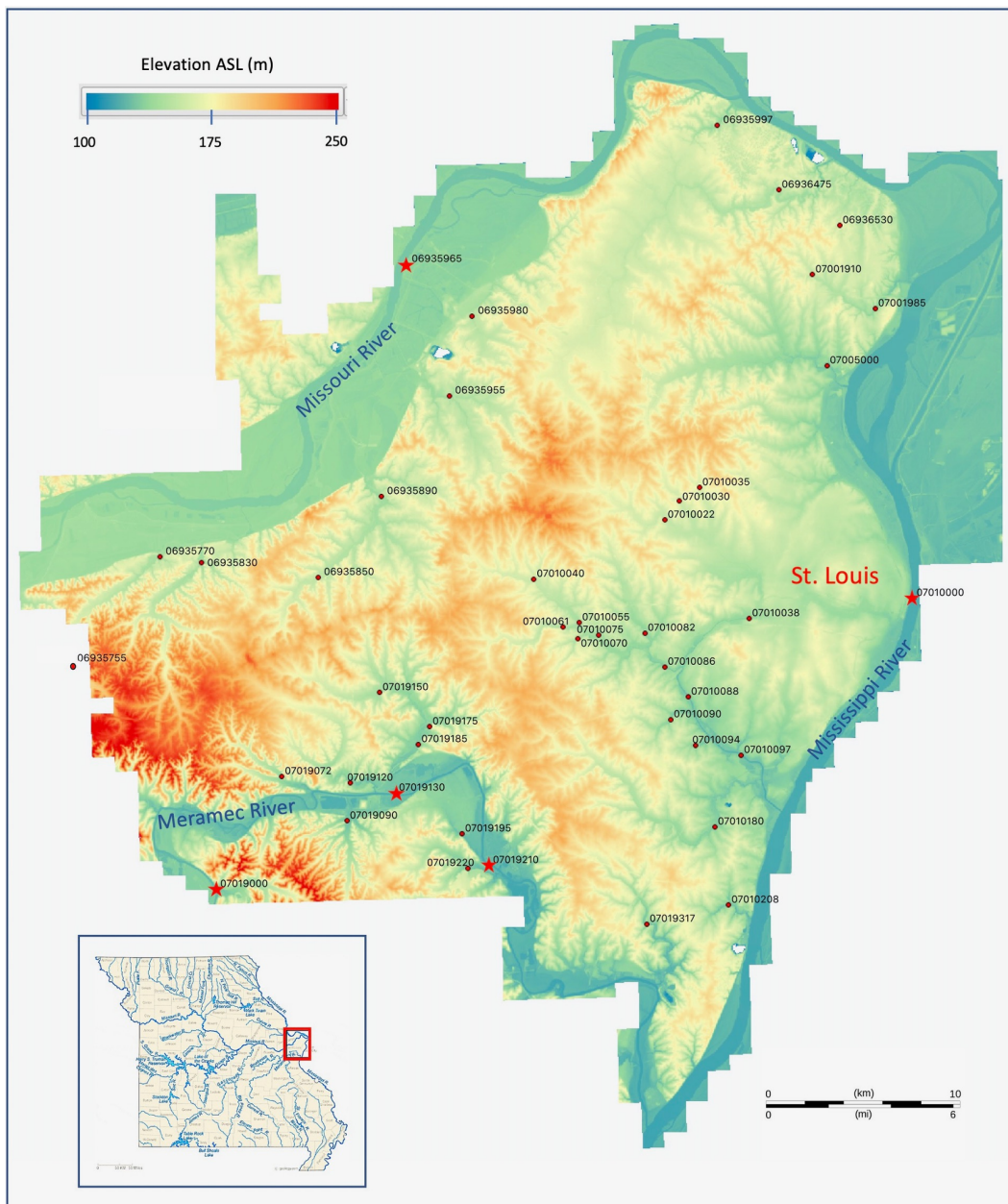
Figure 1. LiDAR map of the St. Louis area, showing regional topography, the locations of gauging stations on creeks that are analyzed in this study (numbered dots), and the additional gauging stations on large rivers (stars). Data from MSDIS (2019); inset map of Missouri modified after https://geology.com/.

2   GENERALIZED DISCHARGE-STAGE RELATION-SHIPS

The rational equation is an exact descriptor of stream discharge

$$Q = A \cdot V_{avg} \tag{1}$$

where Q (m³/s) is the flow rate, A (m²) is the cross-sectional area of the flowing channel, and V_{avg} (m/s) is the average velocity of the flow. Unfortunately, none of the quantities in this equation are easy to measure, particularly to good accuracy in natural streams. Thus, it is imperative to relate each of these quantities to the easily measured water level. For example, many equations for weirs establish relationships between discharge and level above the weir invert (e.g., Chow, 1964).

Similarly, Criss (2020) showed that a relationship that closely resembles the equation for a triangular weir

$$Q = a(h_L - h_o)^n \tag{2}$$

provides a good description of discharge measurements at most gauging stations along the Missouri and Mississippi rivers. Here, a is a constant that has no value as a comparative metric as its units vary from site to site, whereas n is a dimensionless power with physical significance. Analogous equations, but with different multiplicative constants b and c and different dimensionless powers m and p, were shown to describe measurements of channel area and average water velocity at the same sites (see Eqs. 5 and 6, below). Here, h_L is the local stage in meters that is typically referenced to an arbitrary datum, while h_o represents the effective level of the channel bottom. The difference between these quantities, h^*, is a physically-meaningful metric representing water depth, that equates to zero discharge when h^* is zero, because the channel is effectively dry (e.g., De Wiest, 1965).

3   METHODS AND DATA

Understanding the dynamics of flash floods is a worthy goal of hydrologic science. Central to this effort is a theoretical understanding of the discharge-stage relationship. We have developed several novel techniques to further this understanding, and in particular to determine n and h_o in Eq. 2 from available data, as described below.

3.1   Available Data

The USGS (2020) continuously monitors 39 gauging stations on small streams in the St Louis area, emphasized below, as well as a few long-term sites on the much larger Mississippi, Missouri, and Meramec rivers. Of the 39 sites, 26 have operated since about 1997, and only three (07010038, 07010040, 07010088) have less than 10 years of record.

Detailed rating tables are available for each of these sites (USGS, 2020). These provide the USGS calibration of discharge for the measured stage, with values tabulated every 0.01 foot (3 mm).

Collectively, the USGS has conducted 9 039 individual site visits to calibrate and routinely update the 39 rating tables for the small creeks. Summaries of the underlying "field measurements" made during each of these site visits are also accessible on pages available through USGS (2020). These summaries include the date, local stage, estimated discharge, the

method used, and commonly also the width, area and average velocity of the wet channel. Unfortunately, many of the measurements of width, area and velocity that underlie each discharge estimate are made, for convenience or necessity, at a considerable but variable distance from the gauge where stage is recorded. While this procedure has little effect on the estimated discharge at the gauge, it can greatly affect the separate determinations of area and velocity, but not their product Q, because channel character can vary appreciably along small streams. Also, the USGS (2020) provides a somewhat subjective assessment of the reliability of the discharge estimate made during each site visit, with most estimates being rated by them as "poor". An important detail is that the discharge measurements on small creeks are heavily weighted to small discharges, so the calibration during high flow conditions is poorly constrained (Fig. 2).

Finally, a detailed LiDAR survey from the USGS 3DEP elevation program is available for practically all of the St. Louis region (MSDIS, 2019), covering 1 621 km² (626 square miles) and all but one of the gauged sites (06935755). The LiDAR-based product "is a hydro-flattened, topographic bare-earth raster DEM, with a 1 m² cell size and a 10 cm root mean square error (RMSE) threshold for vertical accuracy" (Arundel et al., 2015; NOAA, 2012). The data are referenced to the NAD83 horizontal datum and the NAVD88 vertical datum (Arundel et al., 2015). The aerial surveys of the St. Louis region were made during very low flow conditions on Feb. 17–20 and Feb. 27, 2017 (Surdex, 2017), so creek bottoms were all but dry (cf., USGS, 2020), and the bottoms of their channels could be imaged. Where we have compared the LiDAR elevations to benchmarks we find that accuracy is better than ±0.3 m, and suggest that relative differences on a local scale are smaller.

3.2   Method 1

A simple graphical technique can be applied to the USGS field measurements that provide stage-discharge pairs, to determine unique n and h_o values for individual sites (Criss, 2020). Specifically, if a plot is made of the quantity $Q^{1/n}$ vs. local stage h_L, and then n is iterated from an initial guess, the optimal value of n is indicated when the strongest resultant linear regression is obtained, and the x-intercept of this line directly provides h_o. Criss (2020) applied this technique to 27 long-term gauging stations along the Madison-Missouri-Mississippi River System, finding an average $n=2.57\pm0.64$. For example, for data collected during 3 583 different site visits to the Mississippi River at St. Louis (gauge #07010000), he determined that $n=2.35$ and $h_o=$ -7.0 m, with the latter value comparing closely with the bathymetrically- defined channel bottom.

3.3   Method 2

The graphical technique of Method 1 can also be applied to the USGS rating tables that are available for individual sites (USGS, 2020). These rating tables use hundreds of points that are closely and evenly spaced to depict a smooth relationship between discharge and stage; moreover, the tables are routinely updated to reflect current conditions. Thus, the values in these tables differ from the field data on which they are based. For example, field data are typically collected at unevenly spaced

stages, at variable intervals that collectively span many years, during which channel conditions can change. Also, as discussed above (Fig. 2), discharge calibration is poor for high flows.

3.4   Method 3

We developed a mathematical method that directly yields n and h_o from Eq. 2. Analytical solutions to inverse problems in the physical sciences are uncommon, and the underlying logic is unfamiliar and little taught (Groetsch, 1999), but the simplicity of Eq. 2 renders one possible. Specifically, the derivative of Eq. 2 can be expressed in a manner that eliminates the constant a

$$dQ/dh_L=na(h_L-h_o)^{n-1}=na(h_L-h_o)^n/(h_L-h_o)=nQ/(h_L-h_o) \quad (3)$$

Rearranging gives

$$h_L=h_o+nQ/(dQ/dh_L) \quad (4)$$

Thus, a plot of h_L vs. Q divided by dQ/dh_L directly provides a line of slope n and y-intercept h_o. Because the points in the rating tables are very closely spaced, trivial numerical methods can accurately define dQ/dh_L at each point along the rating curve. As shown below, the USGS rating tables in the St. Louis region indeed define strong linear relationships on such a graph.

3.5   Method 4

We developed a final method to use Eq. 1 to predict the dependence of discharge on stage, in a manner that is entirely independent of USGS stream data. This method utilizes high resolution LiDAR data that are available for almost all of the St.

Louis region, to define the topographic cross-section at or very near each USGS gauging station. Figure 3 shows representative examples of the 39 sites.
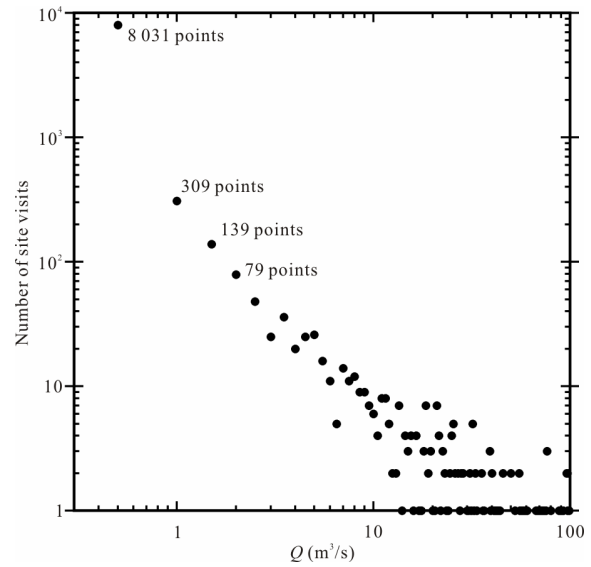
Figure 2. Histogram of discharge estimated during the 9 039 individual site visits made by USGS to St. Louis creeks, plotted on logarithmic axes because the distribution is extremely skewed. Of those visits, 8 031 (88.8%) were conducted when discharge was <0.5 m³/s, 8 863 (98%) when discharge was <12 m³/s, and only 14 visits (0.15%, off-scale) were conducted when flows exceeded 100 m³/s. Data from USGS (2020).
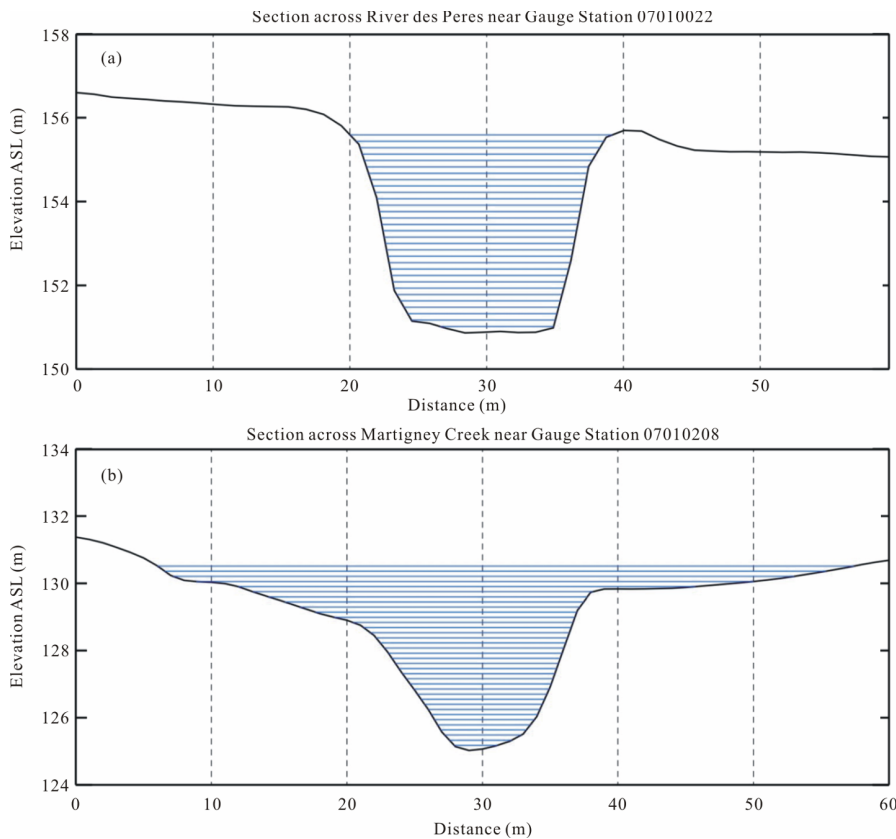
Figure 3. Example cross-sections of the creeks at gauging stations 07010022 and 07010208, made from LiDAR data. The horizontal lines represent ½ foot (15.2 mm) depth intervals from which channel area and hydraulic radius were determined for use in calculating their dependence on stage.

These sections were processed to determine the channel bottom elevation h_o, as well as the dependencies of the channel area and hydraulic radius on the stage. Specifically, we find that the channel area can be depicted with good to excellent accuracy by

$$A = b(h_L - h_o)^m \qquad (5)$$

and that, using the Manning Equation, the relationship for a triangular weir, or the analysis of Criss (2020) for large rivers, the average channel velocity can be depicted to good accuracy by

$$V_{\mathrm{avg}} = c(h_L - h_o)^p \qquad (6)$$

where b and c are site-specific constants with variable units, and m and p are dimensionless powers. Comparing these results to Eq. 1, it is evident that $n = m+p$. Importantly, here h_o and m are defined by LiDAR data, and p is defined by empirical or theoretical relationships. Thus, Method 4 provides results for the discharge-stage relationship that are entirely independent of data from the flowing stream at each specific site.

LiDAR methods are being increasingly investigated for altimetry-based stream monitoring and to establish the relationship between stream stage and discharge (e.g., Paul et al., 2020; Madin and English, 2012). However, these studies typically measure the elevation of the water surface rather than the dry stream shape and bottom elevation, and require repeated LiDAR scans over a period of time to adequately sample different stream stages. Nathanson et al. (2012) describe a method to determine rating curves using LiDAR data to define channel geometry in a fluid mechanics-based model. Neither of these approaches have the operational and mathematical simplicity of Method 4, which derives the key parameters that characterize a given site along a stream.

4   RESULTS

4.1   Analysis of Methods 1–3

Table 1 provides the results for the application of the four aforementioned methods to each of the 39 sites. The average value returned for dimensionless n when "Method 1" is applied to the field data is 1.821±0.38, which is considerably smaller than the average of 2.57±0.64 that Criss (2020) found for 27 gauging stations along the much larger Madison, Missouri, and Mississippi rivers. The correlation coefficients of the trend lines for the 39 sites have an average $R^2 \sim 0.889$, which is lower than that found for the large river sites.

Results are more consistent when the same graphical technique is applied to the rating tables (Method 2). The average returned value for n is 1.893±0.37, but with $R^2 > 0.994$ at all 39 sites. Interestingly, although this average value for n is almost identical to that returned for the field data (Method 1), the agreement of values for individual sites is fair to poor (Fig. 4).

In contrast, the Method 2 values agree well with the purely mathematical inverse Method 3, which returns a similar average value for n of 1.868±0.36, with the trend lines for all but 5 sites having $R^2 \geq 0.976$. Those 5 sites, particularly #07019090, exhibited large and abrupt discontinuities in the trends on Method 3 graphs. Importantly, with those few exceptions the values of n determined for the rating tables by Method 3 agree well with those determined by Method 2 (Fig. 4). This agreement lends mathematical support to the robustness of methods

1 and 2. Moreover, the strong linearity of the Method 3 trend lines shows that the USGS rating tables at these sites do indeed closely resemble the power relationship of Eq. 2.

4.2   Analysis of Method 4

Method 4 provides a means to use LiDAR data and other arguments to predict values for n and h_o for 38 of the 39 sites, entirely independently of USGS stream data. These data were used to construct topographic cross sections of the channel at or very near the gauging stations, which were processed to determine the dependences of channel area and hydraulic radius on h^*. The same graphic technique used in Method 1 was then applied to these LiDAR profiles to determine power m and level h_o in Eq. 5, and of analogous power q and h_o for hydraulic radius. In the few cases where the channel is engineered to have vertical concrete walls, these LiDAR sections can appear to be smoother than they actually are, which can cause a small increase of <0.2 in the apparent value of m over the actual unit value. According to the Manning Equation, power p for velocity (Eq. 6) should equal $2q/3$; alternatively, Criss (2020) found that p was 1.02±0.28 for the river sites he examined. If the various power relationships are reasonably robust and values for h_o are either reasonably consistent or required to be identical, Eq. 1 requires that $n = m+p$.

The average value of m of the 38 sites for which LiDAR data are available was 1.550±0.286, while that for q was 0.890±0.228. The former compares very closely with the value of 1.55±0.48 that Criss (2020) found for the 27 river sites he examined, and closely approximates the exact power of 3/2 for a parabolic channel. It follows that the average value of $n = m+p$ predicted by this method should be about 2.14 if the Manning Equation is used to estimate p, or about 2.57 if Criss' result of $p \sim 1.0$ for the mid western rivers is used. In either case these predicted values of n are significantly higher than those provided by the USGS field data and rating tables for the small streams (Fig. 5). Note in these comparisons that the standard deviations attached to the various averages are statistical descriptors of the differences among the 27 to 39 sites being discussed, and are not "errors" in the average values.

4.3   Assessment of USGS Data

The discrepancies outlined above warrant critical examination of the USGS field measurements made during the 9 039 different site visits to St. Louis creeks, and of the rating tables derived from them. Several means to do this are available.

First, the data base reveals that the mean discharge estimated during the 9 039 site visits was only 1.42 m³/s (50 cfs), and because the distribution of values is strongly skewed, the median estimated flow was only 0.04 m³/s. Flows exceeded 30 m³/s (1 060 cfs) during only 1% of site visits (Fig. 2). To place these flows in context, urban flooding at most of the 39 sites becomes significant when estimated flows exceed 50–300 m³/s, yet practically all measurements were made under low flow conditions, when $h^* < 25$ cm.

As an example, consider site 07010022, chosen because the September 2008 flash flood caused two fatalities only 0.6 km upstream of this station (Wilson, 2009). During this flood, a water depth of 4.3 m above channel bottom was attained, with

**Table 1**   Estimates[1] of power *n* for gauged sites on St. Louis creeks

Site #	Creek name	Catchment area (km²)	*n* from field data	*n* from rating curve	*n* from inverse	*m*+1	*m*+2*q*/3
06935755	Bonhomme	11.5	(1.140)	2.196	(2.058)		
06935770	Bonhomme	29.3	2.160	2.100	2.101	3.228	2.773
06935830	Caulks	44.3	(1.528)	1.900	1.983	2.566	2.166
06935850	Creve Coeur	14.6	(2.210)	2.022	2.044	3.138	2.797
06935890	Creve Coeur	57.0	(1.976)	2.088	2.123	2.452	(2.007)
06935955	FeeFee	30.3	(1.332)	1.670	1.770	2.596	(2.056)
06935980	Cowmire	9.7	2.114	2.118	2.176	2.394	(1.993)
06935997	Mill	5.5	0.970	1.192	1.180	3.162	2.995
06936475	Coldwater	104.6	1.618	1.356	1.351	2.436	2.220
06936530	Spanish Lake	0.65	(2.080)	2.244	2.325	2.916	(2.944)
07001910	Watkins	2.98	(1.050)	2.146	2.230	2.864	(2.307)
07001985	Watkins	13.4	(1.954)	1.820	1.857	2.454	(2.058)
07005000	Maline	63.2	(1.810)	1.520	1.546	2.372	1.896
07010022	RDP[2]	23.2	1.536	1.568	1.585	2.202	1.663
07010030	RDP[2] Trib.	5.21	(2.940)	2.150	2.249	2.402	1.857
07010035	Engelholm	3.63	1.970	2.184	2.200	2.322	1.887
07010038	RDP[2]	73.3	1.392	1.550	1.601	2.534	2.045
07010040	Denny	1.24	(1.684)	1.736	1.517	2.490	1.875
07010055	Deer	31.1	1.892	1.884	1.893	2.708	2.351
07010061	Two Mile	16.7	(1.896)	2.392	2.509	2.164	1.716
07010070	Sebago	4.84	(1.846)	1.530	1.561	2.480	2.068
07010075	Deer	55.4	1.608	1.908	(1.998)	2.666	2.425
07010082	Black	15.1	(1.750)	1.338	1.258	2.160	1.683
07010086	Deer	94.5	2.008	1.948	1.940	2.532	2.121
07010088	RDP[2]	185.4	1.850	1.830	1.726	2.164	1.747
07010090	MacKenzie	9.04	(1.808)	1.780	1.776	2.886	3.033
07010094	Grammond	1.61	(2.358)	2.266	2.257	2.560	2.041
07010097	RDP[2]	220.7	(2.170)	2.098	2.227	2.158	1.745
07010180	Gravois	46.88	(1.790)	1.694	1.738	2.370	1.826
07010208	Martigney	6.84	1.784	1.806	1.815	2.998	(2.658)
07019072	Kiefer	10.1	1.530	1.616	1.613	2.518	(2.091)
07019090	Williams	19.7	(1.718)	3.124	(2.383)	2.340	1.881
07019120	Fishpot	24.8	(1.766)	2.052	(2.201)	2.334	1.839
07019150	Grand Glaize	13.2	1.916	2.014	1.940	2.342	1.885
07019175	Sugar	13.2	(2.624)	1.968	1.824	2.526	(2.175)
07019185	Grand Glaize	56.6	1.526	1.390	1.117	2.634	2.273
07019195	Yarnell	7.02	(2.026)	2.348	2.353	2.868	(2.292)
07019220	Fenton	11.1	(1.854)	1.280	1.209	2.672	(2.277)
07019317	Mattese	20.4	1.836	2.012	2.020	2.286	1.783

[1]. Numbers in parentheses have $R^2<0.95$; *m*+1 and *m*+2*q*/3 are two estimates for *n*; [2]. RDP, River des Peres.

an estimated flow of 143 m³/s. For comparison, of the 263 different USGS site visits used to calibrate this site, only 14 had estimated flows >2.8 m³/s, and only one exceeded 32 m³/s (Fig. 6a), yet flows above 65 m³/s occur every year (USGS, 2020). The single high-water discharge estimate, 125 m³/s for a water depth of ~4.0 m, was made by indirect method "QIDIR" with neither channel width, channel area, nor average velocity being reported (USGS, 2020). In short, more than 90% of the USGS field measurements at this site were made when water levels were less than 0.25 m above the channel bottom, and the calibration relevant to flooding is virtually nonexistent. Yet, the USGS rating table for this site provides discharge estimates at 3 mm intervals, up to flows of 169 m³/s, and would appear to a casual reader to be very well constrained (Fig. 6b). Clearly, the distribution of points in Fig. 6a provides little support for the curve, particularly given that the single point at high flow was estimated by an unspecified, indirect procedure.

A final comparison can be made of the elevations of the channel bottom, as respectively indicated by the USGS gauge datums corrected by the stage corresponding to zero discharge in their rating tables, and the channel bottom indicated by LiDAR (Fig. 7). These compare poorly, regardless of whether the
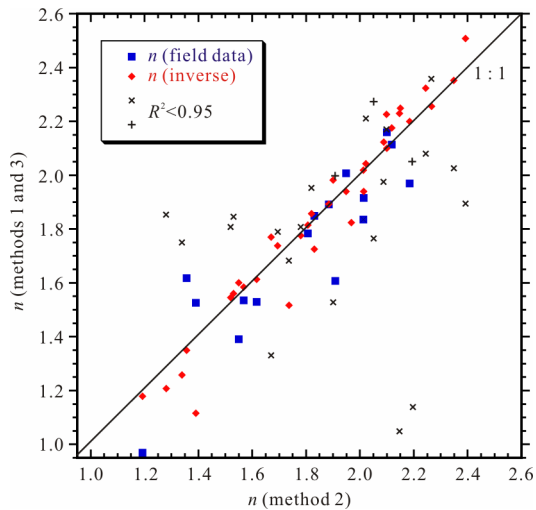
Figure 4. Scatter plot of values of *n* determined from field data (Method 1) and from the mathematical inverse method (Method 3), compared to values determined by Method 2 processing of rating tables. Open symbols (×, +) depict scattered results for sites where the correlation coefficients for the Method 1 or 3 determinations were lower than 0.95.
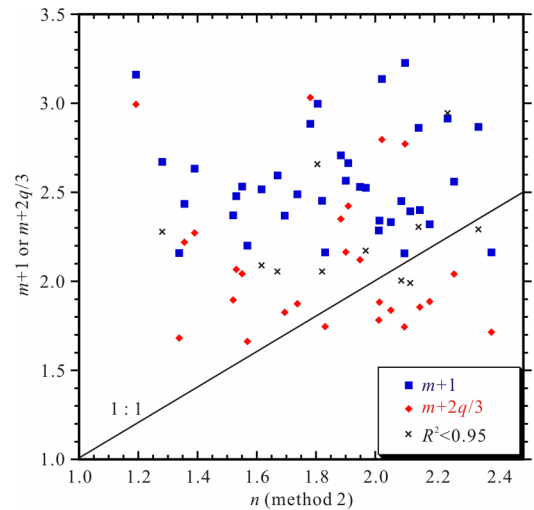
Figure 5. Two estimates of *n*, independently provided by LiDAR plus empirical (*m*+1) and LiDAR plus Manning (*m*+2*q*/3) relationships (Method 4), plotted against the value of *n* determined by Method 2 processing of rating tables. The LiDAR-based values tend to be higher than values determined from the rating tables, regardless of whether the Manning or the Criss proportionalities for average water velocity are used.
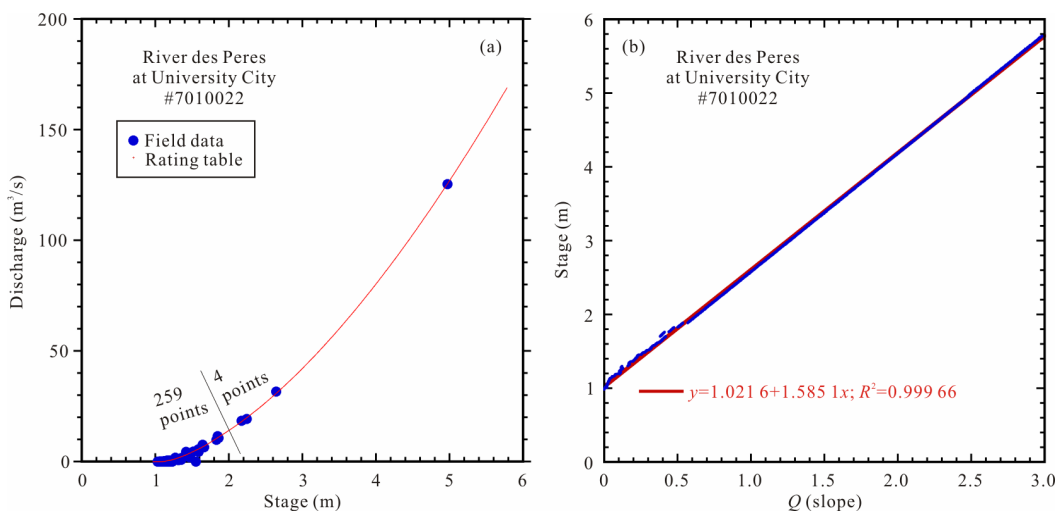
Figure 6. Relationships for the upper River des Peres at University City. (a) Comparison of field measurements (blue dots) with the hundreds of entries in the current USGS rating table for this site, whose closely spaced data points (tiny red dots) appear to depict a smooth continuous curve. (b) Method 3 analysis of the entries in the USGS rating table (tiny blue dots) provides a value of 1.02 m for h_o, and a value for *n* of 1.58 (see text).

small correction (average 0.35 m) is applied to the LiDAR data to correct for the h_o estimates indicated by our area *vs*. stage plots. For the 38 sites, the average absolute difference between the USGS and LiDAR channel bottom elevations is 0.95 m; and the differences in elevation exceed 2.0 m for 7 sites, of which two exceed 4.5 m (sites 06935997; 07010094).

5   DISCUSSION

The dynamics of small streams are very interesting, as they respond much more rapidly to heavy rainfall than do rivers, and quickly rise to water depths that are almost as great. The time constants of urban creeks are further shortened because flow delivery is accelerated by impervious surfaces and storm sewers, so their flash floods are frequent and severe. However, for many reasons including their irrelevance to navigation, very few sites with long-term gauging records are located on creeks. It follows that monitoring small streams and understanding their dynamics are significant research opportunities. This includes monitoring of small streams in natural and rural areas, to provide a baseline for understanding their urbanized counterparts.

We are disappointed that our attempt to glean information from the St. Louis database on small streams provided rather disparate results among the several methods we devised. Part of this problem originates in inaccuracies in the discharge estimates themselves, and in the rarity of relevant measurements under high flow conditions. Making hundreds of determinations on streams that are a few inches deep has little relevance to the important issues and hazards at hand. Far more attention should also be directed into providing accurate gauge datums for the sites, and the drainage areas that contribute flow, which
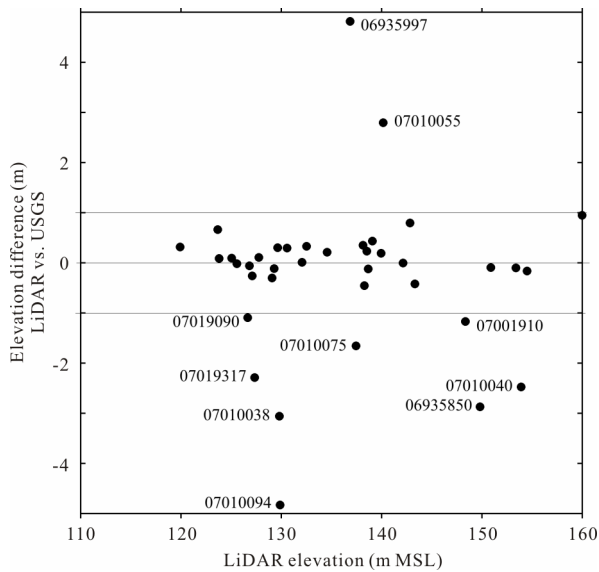
Figure 7. Graph of the difference between channel bottom elevations determined from LiDAR data and from USGS rating tables and gauge data, plotted against the LiDAR elevation. Horizontal reference lines are shown for differences of -1, 0 and +1 m; station numbers are indicated for stations whose differences exceed ±1 m.

in some cases appear to be taken from FEMA tables that commonly list values for ambiguous locations (e.g., FEMA, 2015).

We discourage the use of hydraulic radius, the venerable variable representing channel area divided by wet perimeter, as a metric of hydraulic conditions. First, that quantity is difficult to measure, and to our knowledge, is never reported for streams. Second, hydraulic radius has no simple relationship to stage, even for geometrically simple channels such as one with perfectly rectangular or parabolic shapes. Third, if surfaces are truly fractal, the length of the wetted perimeter is scale dependent and becomes very large with increasingly detailed view, rendering the hydraulic radius an inconsistent measure of channel character. Fourth, for the LiDAR cross sections we defined, the correlation between hydraulic radius and stage was far weaker than the almost perfect relationships we obtained for each section between channel area and stage. Finally, regarding the Manning Equation itself, Criss (2020) found little support for its alleged proportionalities, and in fact Chow (1964) tabulated a long list of proposed relationships between average channel velocity and hydraulic radius that depend on a wide range of powers.

The techniques we have developed have broad applicability to free-flowing streams at stages within their banks. This is demonstrated by the results at the large number of sites investigated in this and our companion study, by the large range in the hydrologic character of those sites, and by our spot checks of results at many other gauging stations. While we have assumed that Eq. 2 is a good or excellent descriptor of the discharge-stage relationship, Method 3 provides a rapid method to check whether this assumption is accurate at any given site, and this property alone provides general utility. We have also shown how these graphical and mathematical methods can be used to further understanding of the physical laws that govern the discharge-stage, velocity-stage, and area-stage relationships in real streams.

Finally, our findings provide no support for the statistical

analysis of historical discharge tables (USGS, 1981) to estimate flood frequency, severity or risk. Multiple papers (e.g., Criss, 2020, 2016; Criss and Luo, 2017) provide a long list of reasons why stage is the parameter most relevant to flood risk, particularly because it is readily observable, easily measured, and directly relevant to flood damage. Those identified reasons did not include the conclusion of this paper, that discharge is a dependent variable that is poorly calibrated in small urban watersheds, but direct and accurate measurement of stage is routine.

6 CONCLUSIONS

Available stream flow and LiDAR data from 39 gauging stations on small streams in the St. Louis region, all draining catchments of 0.6 to 220 km^2, provide insights into the dependence of discharge on stage, and into the limitations of the underlying database. Four different techniques were used to extract the optimal power n that relates discharge to water depth, assuming a simple power relationship. Two methods based on rating tables have good mutual agreement, and exhibit strong trends which greatly support the assumed power relationship. However, at most sites the values of n derived from rating tables do not agree well with n derived directly from field data. Prediction of n from LiDAR data on channel shape, combined with the Manning Equation or relationships for large midwestern rivers, do not agree well with n derived from either the USGS field data or the rating tables, suggesting that the latter values are underestimated. The underlying reason appears to be that 90%–98% of USGS field measurements are made under low flow conditions, so behaviors relevant to moderate flows and flooding are not well documented on small streams, and rating tables are poorly calibrated.

REFERENCES CITED

Arundel, S. T., Archuleta, C.-A. M., Phillips, L. A., et al., 2015. 1-Meter Digital Elevation Model Specification. U.S. Geological Survey Techniques and Methods, Book 11, Chapter B7. 25. https://doi.org/10.3133/tm11B7

ASCE, 1988. The River des Peres: A St. Louis Landmark. http://sections.asce.org/stlouis/History/files/River%20des%20Peres%20%20A%20St.%20Louis%20Landmark.pdf

Chow, V. T., 1964. Handbook of Applied Hydrology. McGraw-Hill, New York

Criss, R. E., Lippmann, J. L., Criss, E. M., et al., 2007. Caves of St. Louis County, Missouri. *Missouri Speleology*, 45(1): 1–18

Criss, R. E., 2016. Statistics of Evolving Populations and Their Relevance to Flood Risk. *Journal of Earth Science*, 27(1): 2–8. https://doi.org/10.1007/s12583-015-0641-9

Criss, R. E., Luo, M. M., 2017. Increasing Risk and Uncertainty of Flooding in the Mississippi River Basin. *Hydrological Processes*, 31(6): 1283–1292. https://doi.org/10.1002/hyp.11097

Criss, R. E., 2018. Theoretical Link between Rainfall and Flood Magnitude. *Hydrological Processes*, 32(11): 1607–1615. https://doi.org/10.1002/hyp.11511

Criss, R. E., 2020. Dependence of Discharge, Channel Area, and Flow Velocity on River Stage and a Refutation of Manning's Equation. In: Foulger, G. R., Jurdy, D. M, Stein, C. M., et al., eds., In the Footsteps of Warren B. Hamilton: New Ideas in Earth Science, Geological Society of America Special Paper

De Wiest, R. J. M., 1965. Geohydrology. John Wiley & Sons, New York

FEMA, 2015. Flood Insurance Study, St. Louis County, Missouri. Volumes 1–4. Study No. 29889CV001A

Groetsch, C. W., 1999. Inverse Problems: Activities for Undergraduates. Cambridge University Press, Cambridge

Harrison, R. W., 1997. Bedrock Geologic Map of the St. Louis 30'×60' Quadrangle, Missouri and Illinois. U.S. Geological Survey, Miscellaneous Investigations Series, Map I-2533

Hasenmueller, E. A., Criss, R. E., 2013. Multiple Sources of Boron in Urban Surface Waters and Groundwaters. *Science of the Total Environment*, 447: 235–247. https://doi.org/10.1016/j.scitotenv.2013.01.001

Lutzen, E. E., Rockaway, J. D. Jr., 1989. Engineering Geologic Map of St. Louis County, Missouri. Missouri Dept. of Natural Resources. OFM-89-256-EG

Madin, I., English, J. T., 2012. Interpolating Stage-Discharge Relationships Using Serial LiDAR along the Sandy River, Oregon. AGU Fall Meeting Abstracts, G23A-0898

MODNR, 2020. List of Impaired Waters (303d). Missouri Department of Natural Resources. https://dnr.mo.gov/env/wpp/waterquality/index.html

MSDIS, 2019. Missouri Spatial Data Information Service. (2019-11) [2020-10-9] http://msdis.missouri.edu/data

Nathanson, M., Kean, J. W., Grabs, T. J., et al., 2012. Modelling Rating Curves Using Remotely Sensed LiDAR Data. *Hydrological Processes*, 26(9): 1427–1434. https://doi.org/10.1002/hyp.9225

NWS, 2020. NWS Forecast Office St. Louis, MO. https://www.weather.gov/lsx/

National Oceanic and Atmospheric Administration (NOAA) Coastal Services Center, 2012. Lidar 101: An Introduction to Lidar Technology, Data, and Applications. Revised. NOAA Coastal Services Center, Charleston, SC

NOAA, 2017. Atlas 14 Point Precipitation Frequency Estimates: Missouri. [2020-6-1]. https://hdsc.nws.noaa.gov/hdsc/pfds/pfds_map_cont.html

Paul, J. D., Buytaert, W., Sah, N., 2020. A Technical Evaluation of LiDAR-Based Measurement of River Water Levels. *Water Resources Research*, 56(4): e2019WR026810. https://doi.org/10.1029/2019wr026810

Southard, R. E., 2010. Estimation of the Magnitude and Frequency of Floods in Urban Basins in Missouri. USGS Scientific Investigations Report 2010-5073. 27

Surdex, 2017. St. Louis LiDAR Acquisition and Processing Report; LiDAR Flight Log Report; USACE Contract G16PC00029

USGS, 1981. Guidelines for Determining Flood Flow Frequency. Interagency Advisory Committee on Water Data, Bulletin #17B of the Hydrology Subcommittee. U.S. Geological Survey, Office of Water Data Coordination, Reston, Virginia

USGS, 2020. USGS Current Water Data for Missouri. (2020-5). https://waterdata.usgs.gov/mo/nwis/rt

Vineyard, J. D., 1967. Physiography. In: Mineral and Water Resources of Missouri. Missouri Division of Geological Survey and Water Resources, 43: 13–15

Wahl, K. L., Thomas, W. O. Jr., Hirsch, R. M., 1995. Stream-Gaging Program of the US Geological Survey. US Geol. Survey Circular 1123, Reston, Virginia. http://water.usgs.gov/pubs/circ/circ1123

Wilson, D. A., 2009. Hurricane Ike and Impact of Localized Flooding in St. Louis County, Sept. 14, 2008. In: Criss, R. E., Kusky, T. M., eds., Finding the Balance between Floods, Flood Protection, and River Navigation. St. Louis University, Center for Environmental Sciences, St. Louis. 22–27